Digital Life: Satisfying Seven Biological Criteria Through Functional Analogy and Criterion-Ablation

Anonymous

Abstract

We present a testable integration of all seven textbook biological criteria for life—cellular organization, metabolism, homeostasis, growth, reproduction, response to stimuli, and evolution—as functionally interdependent computational processes within a single artificial life system. Existing systems implement at most a subset of these criteria, often as independent modules or static proxies that can be removed without measurable system degradation. Our hybrid swarm-organism architecture implements each criterion as a dynamic process satisfying three conditions—sustained resource consumption, measurable degradation upon removal, and feedback coupling with other criteria—which we term functional analogy. A criterion-ablation experiment (n=30 per condition, seeds held out from calibration) demonstrates that disabling any single criterion causes statistically significant population decline (Mann-Whitney U, Holm-Bonferroni corrected, all $p \leq 0.016$), with Cliff's δ ranging from 0.18 to 1.00. Pairwise ablations reveal sub-additive interactions consistent with shared failure pathways, confirming that criteria damage overlapping subsystems rather than operating independently. A proxy control comparison shows that metabolism implementations of differing complexity produce qualitatively distinct population dynamics, ruling out tautological criterion definitions. The strongest single-ablation effects arise from disabling reproduction (Δ=–89.3%), response to stimuli (Δ=–88.4%), and metabolism (Δ=–84.3%), confirming that these criteria function as necessary, interdependent components of organismal viability rather than decorative labels.

Introduction

What distinguishes a living system from a merely complex one? Biology textbooks identify seven criteria—cellular organization, metabolism, homeostasis, growth and development, reproduction, response to stimuli, and evolution (Urry et al., 2020)—but artificial life (ALife) research has struggled to integrate all seven into a single computational system. Most existing platforms implement a subset: evolutionary dynamics without metabolism (Ofria and Wilke, 2004), pattern formation without reproduction (Chan, 2019), or boundary self-organization without evolution (Plantec et al., 2023). Where criteria are nominally present, they often function as simplified proxies—static parameters or independent modules whose removal has no measurable effect on system behavior.

We argue that a meaningful computational model of life requires more than feature checklists. Each criterion must function as a functional analogy of its biological counterpart, satisfying three conditions:

1. Dynamic process: the criterion requires sustained resource consumption at every timestep, not a static lookup.

2. Measurable degradation: ablating the criterion causes statistically significant decline in organism viability.

3. Feedback coupling: the criterion forms at least one feedback loop with another criterion, precluding independent-module implementations.

This definition operationalizes the intuition behind autopoiesis (Maturana and Varela, 1980) and minimal-life frameworks (Ruiz-Mirazo et al., 2004) in a form amenable to experimental falsification.

We adopt a weak ALife stance: our system is a functional model of life, not a claim that the organisms are alive. The contribution is methodological—demonstrating that all seven criteria can be integrated as interdependent processes and that their necessity can be rigorously tested.

This paper makes four contributions:

1. A hybrid swarm-organism architecture integrating all seven biological criteria as functionally interdependent processes.

2. An operational definition of functional analogy with three falsifiable conditions.

3. A criterion-ablation methodology demonstrating each criterion's functional necessity via controlled experiments with multiple-comparison correction.

4. Pairwise ablation and proxy control experiments characterizing criterion interactions and ruling out tautological definitions.

Related Work

Artificial life research has produced diverse computational substrates, each excelling along different axes of biological fidelity. We organize the landscape by methodological approach rather than chronology.

Evolutionary platforms. Tierra (Ray, 1991) and Avida (Ofria and Wilke, 2004) pioneered self-replicating digital organisms with mutation and natural selection, achieving strong evolutionary dynamics (Level 5 on our rubric). However, organisms lack spatial bodies, metabolic processes, and boundary maintenance—criteria 1–4 receive minimal or no implementation. Polyworld (Yaeger, 1994) adds neural-network-driven behavior and simple energy budgets, though its metabolism operates as a dynamic single-resource process rather than a multi-step network.

Continuous and particle-based systems. Lenia (Chan, 2019) demonstrates emergent lifelike patterns in continuous cellular automata, exhibiting coherent spatial organization and growth. Flow-Lenia (Plantec et al., 2023) extends this with mass conservation, achieving stronger boundary maintenance. ALIEN (Heinemann, 2008) provides a GPU-accelerated particle simulator with typed cells supporting self-replicating structures, achieving multi-process interaction on several criteria. While ALIEN demonstrates broad coverage, no existing system combines multi-step metabolism with active homeostatic regulation.

Chemistry-inspired systems. Coralai (Barbieux and Canaan, 2024) combines multi-agent neural cellular automata with energy dynamics, implementing rudimentary metabolism and spatial organization. It represents a step toward metabolic integration but does not achieve the feedback coupling between metabolism and other criteria that our framework requires.

Theoretical foundations. The autopoiesis framework (Maturana and Varela, 1980; McMullin, 2004) emphasizes self-producing boundaries as the minimal criterion for life, which our boundary-maintenance mechanism operationalizes. NASA's working definition—"a self-sustaining chemical system capable of Darwinian evolution" (Joyce, 1994)—bundles metabolism and evolution but does not individuate the remaining five criteria. Ruiz-Mirazo et al. (2004) argue for a richer set of minimal conditions, closer to our seven-criteria framework. The open-ended evolution research program (Bedau et al., 2000; Taylor et al., 2016) provides metrics for evolutionary richness that complement our criterion-ablation approach.

Table 1 summarizes how existing systems score on each criterion using a five-level rubric (1=absent, 5=self-maintaining/emergent).

While ALIEN achieves Level 4 on four criteria, it lacks multi-step metabolism (Level 3) and active homeostasis (Level 2). Our system reaches ≥ 4 on five of seven criteria, with the highest total score (26) across all systems surveyed. We note that these scores are self-assessed; independent evaluation may adjust individual ratings.

System Design

Architecture Overview

The system implements a hybrid two-layer architecture (Figure 1). The outer layer is a continuous toroidal 2D environment (100×100 world units) containing a diffusing resource field. The inner layer consists of 10–50 organisms, each composed of 10–50 swarm agents that collectively maintain the organism's spatial boundary.

Each organism maintains the following runtime state: boundary integrity ($b \in [0, 1]$), metabolic state (energy e, resource r, waste w), internal state vector for homeostatic regulation, a neural-network controller, a genetically encoded metabolic network, age, generation counter, and maturity level.

Seven Criteria Implementation

Table 2 maps each biological criterion to its computational implementation, ablation toggle, and feedback partners.

Cellular organization. Swarm agents collectively define an organism's spatial extent. Boundary integrity b decays each step at a base rate modulated by energy deficit and waste pressure: $\Delta b_{\text{decay}} = -r_b \cdot (1 + s_e \cdot (1 - e) + s_w \cdot w)$, where $r_b = 0.02$ is the base decay rate, $s_e = 0.5$ and $s_w = 0.3$ are scaling factors. Repair occurs proportionally to available energy: $\Delta b_{\text{repair}} = r_r \cdot e \cdot (1 - s_p \cdot w)$, with repair rate $r_r = 0.15$ and waste penalty $s_p = 0.4$. When b falls below a collapse threshold ($b < 0.1$), the organism dies.

Metabolism. Each organism possesses a genetically encoded graph-based metabolic network with 2–4 catalytic nodes and directed edges. The genome segment

Table 1: Literature comparison: seven biological criteria scored on a five-level rubric (1=no feature, 2=static parameter, 3=dynamic single process, 4=multi-process interaction, 5=self-maintaining/emergent). Bold indicates scores ≥4.

System	Cell.Org	Metab	Homeo	Growth	Reprod	Response	Evol	Total
Polyworld	2	3	1	1	3	4	4	18
Avida	2	3	1	2	4	3	5	20
Lenia	3	1	2	2	2	3	2	15
ALIEN	4	3	2	3	4	4	4	24
Flow-Lenia	3	3	3	3	3	3	3	21
Coralai	3	3	2	3	3	3	3	20
Ours[†]	4	4	4	3	4	4	3	26

[†]Self-assessment; scores may differ under external evaluation.

Table 2: Mapping of seven biological criteria to computational processes. Each criterion satisfies the three functional-analogy conditions.

Criterion	Process	Feedback
Cell. Org.	Swarm agents maintain boundary; decays without energy	Metab, Homeo
Metabolism	Graph network transforms resources to energy; waste accumulates	Cell. Org., Homeo
Homeostasis	NN regulates internal state vector each step	Metab, Response
Growth	Maturation from seed to full capacity	Metab, Reprod
Reproduction	Division when metabolically ready; energy cost; offspring from seed	Metab, Evol
Response	NN processes sensory input → velocity delta	Homeo, Metab
Evolution	Mutation during reproduction; differential survival	Reprod, all

(16 floats) is decoded via sigmoid mapping: node count = round($\sigma(g_0) \cdot 2 + 2$), catalytic efficiency = $\sigma(g_{2+i}) \cdot 0.9 + 0.1 \in [0.1, 1.0]$, edge existence determined by $|g_j| > 0.3$, and conversion efficiency = $\sigma(g_{13}) \cdot 0.7 + 0.3 \in [0.3, 1.0]$. External resources enter at a designated entry node, flow through the graph with per-edge transfer efficiency in $[0.7, 1.0]$, and exit as energy. Waste accumulates as a byproduct proportional to throughput.

Homeostasis. A feedforward neural network (8 inputs → 16 hidden with tanh → 4 outputs with tanh; 212 weights) processes sensory inputs (position, velocity, internal state, neighbor count) and produces velocity adjustments and internal-state deltas. The internal state vector enables adaptive regulation: organisms that maintain internal variables within viable ranges survive longer.

Growth and development. Organisms begin as minimal seeds (maturity $m = 0$) and develop toward full capacity ($m = 1$) over time. Maturation gates metabolic throughput and reproductive readiness, ensuring organisms must develop before they can reproduce.

Reproduction. When energy exceeds $e_{\min} = 0.7$ and boundary integrity exceeds $b_{\min} = 0.5$, an organism may divide. The parent pays an energy cost ($c_r = 0.3$), and the offspring inherits a (possibly mutated) copy of the genome, starting as a seed. Child agents spawn within a radius of the parent's center of mass.

Response to stimuli. The neural-network controller processes a local sensory field each timestep, producing velocity deltas that govern agent movement. Disabling response freezes agents' velocity adjustments, preventing adaptive resource seeking.

Evolution. During reproduction, offspring genomes undergo point mutations (rate = 0.01 per gene, scale = 0.1), reset mutations (rate = 0.001), and scale mutations (rate = 0.005, factor $\in [0.8, 1.2]$). All gene values are clamped to $[-5, 5]$. This produces heritable variation subject to differential survival.

Genome Encoding

The genome is a variable-length vector of 256 floats organized into seven segments: neural-network weights (212), metabolic network (16), homeostasis parameters (8), developmental program (8), reproduction parameters (4), sensory parameters (4), and evolution parameters (4). All criteria are encoded from initialization; segments are activated as features are enabled.

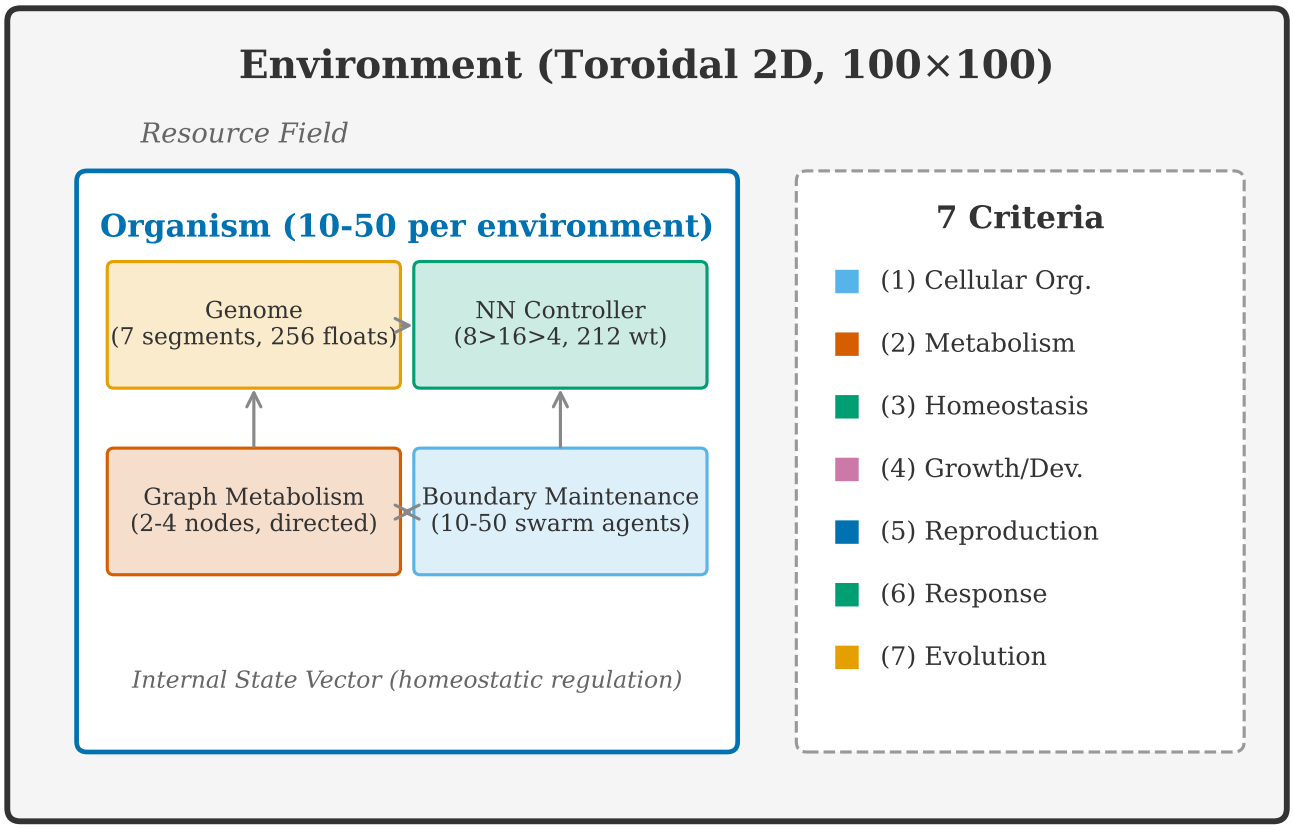

Figure 1: Two-layer architecture. Each organism comprises swarm agents maintaining a spatial boundary, a neural-network controller, a graph-based metabolic network, and a variable-length genome encoding all seven criteria. Organisms inhabit a continuous toroidal environment with a diffusing resource field.

Criterion-Ablation Experiment

This experiment tests whether each of the seven criteria is functionally necessary for organism viability, as predicted by the functional-analogy framework.

Protocol

The system provides seven boolean ablation toggles, one per criterion (e.g., enable_metabolism = false). For each of the seven criteria, we disable that criterion while keeping all others active, and compare the resulting population dynamics against the fully enabled baseline ("normal" condition). This yields eight conditions: one normal baseline and seven single-criterion ablations.

Data Separation

To prevent overfitting of thresholds, we separate data into:

- Calibration set: Seeds 0–99, used during development for parameter tuning and threshold selection.
- Test set: Seeds 100–129 (n=30), held out until final evaluation. All reported results use this set exclusively.

Calibration confirmed that both metabolism engines produce viable populations (Toy: $\bar{x}$=328.1, Graph: $\bar{x}$=291.8 alive at step 2000). All final experiments use the Graph metabolism engine.

Simulation Parameters

Each simulation runs for 2000 timesteps with population sampled every 50 steps. The environment is a 100×100 toroidal grid with 30 initial organisms, each comprising 25 swarm agents. The primary outcome metric is alive organism count at step 2000.

Statistical Design

For each ablation condition, we test the one-sided hypothesis:

$$H_1 : \text{alive\_count}_{\text{normal}} > \text{alive\_count}_{\text{ablated}}$$

Table 3: Criterion-ablation results (n=30 per condition). Normal baseline mean: 293.1 (median: 294, IQR: 283–305). All p-values Holm-Bonferroni corrected. $^{***}p < 0.001$, $^{*}p < 0.05$.

Condition	Mean	Δ%	d	Cliff's δ	p_{corr}	Sig
No Reproduction	31.3	−89.3	18.06	1.00	<0.001	***
No Response	34.1	−88.4	17.82	1.00	<0.001	***
No Metabolism	46.0	−84.3	17.24	1.00	<0.001	***
No Homeostasis	68.3	−76.7	4.94	1.00	<0.001	***
No Boundary	121.8	−58.4	4.36	1.00	<0.001	***
No Growth	185.6	−36.7	5.34	0.97	<0.001	***
No Evolution	278.3	−5.1	0.57	0.18	0.016	*

Table 4: Pairwise ablation synergy scores (n=30 per condition, Graph metabolism). Negative synergy indicates sub-additive interaction (shared failure pathways). Baseline $\bar{x}$=293, consistent with Table 3.

Pair	Δ_{AB}	Expected	Synergy	Ratio
(Metab, Homeo)	249.9	472.0	−222.0	0.53
(Metab, Response)	247.7	506.1	−258.4	0.49
(Reprod, Growth)	261.9	369.4	−107.5	0.71
(Boundary, Homeo)	181.9	396.2	−214.3	0.46
(Response, Homeo)	256.4	483.9	−227.5	0.53
(Reprod, Evol)	261.9	276.7	−14.9	0.95

Ratio = Δ_{AB} / Expected; values <1 indicate shared pathways.

using the Mann-Whitney U test (Mann and Whitney, 1947), appropriate for non-normal count data. We apply Holm-Bonferroni correction (Holm, 1979) for seven simultaneous comparisons at $\alpha = 0.05$. Effect sizes are reported as both Cohen's d (Cohen, 1988) and Cliff's δ (Cliff, 1993), the latter being more appropriate for non-normal distributions. We additionally report the area under the alive-count curve (AUC) and median organism lifespan as secondary outcome measures.

Results

All seven criterion ablations produce statistically significant population decline compared to the normal baseline (Table 3).

Three ablations cause near-total population collapse (>84% decline): reproduction, response to stimuli, and metabolism. These criteria form the core viability loop—without energy production, adaptive movement, or population renewal, organisms cannot sustain themselves.

Figure 2 shows population trajectories across all conditions. The normal condition (black) stabilizes around 293 organisms by step 1000. Metabolic ablation (orange) causes rapid collapse within the first 200 steps, as organisms cannot produce energy to maintain boundaries. Reproduction ablation (blue) produces a slower but equally terminal decline, as the initial population ages and dies without replacement. Evolution ablation (purple) shows the weakest effect (d=0.57), with populations remaining viable but slightly smaller than normal—consistent with evolution operating as an optimization process rather than a survival necessity at these timescales.

Functional analogy verification. For each criterion, all three conditions are satisfied: (a) each consumes resources per step (energy for boundary repair, metabolic computation, NN evaluation); (b) ablation causes significant degradation (Table 3); and (c) feedback loops are observable (e.g., metabolism ↔ boundary: energy funds repair, boundary collapse stops metabolism). Thus, each criterion qualifies as a functional analogy, not a simplified proxy.

Proxy Control Comparison

To test whether criterion ablation merely reflects tautological definitions, we compare three metabolism implementations on the same seeds (n=30): Counter (minimal single-step conversion, no waste), Toy (single-step with waste dynamics), and Graph (full multi-step network with catalytic nodes). All three satisfy "dynamic resource consumption," yet produce qualitatively different dynamics (Figure 3). Graph metabolism supports the highest genome diversity (7.58 vs. 5.69 for Toy) despite sustaining fewer organisms (293 vs. 322 for Toy, 374 for Counter), indicating that metabolic complexity imposes greater selective pressure. This confirms that the specific implementation—not merely the presence—of a criterion shapes system behavior, ruling out tautological definitions.

Pairwise Ablations and Interdependence

To test for interaction effects beyond individual necessity, we disable pairs of criteria and compute synergy: $\text{synergy}_{A,B} = \Delta_{A \cup B} - (\Delta_A + \Delta_B)$. Table 4 reports scores for six pairs. All show sub-additive synergy (negative), indicating shared failure pathways: individual ablations already collapse populations to near their floor (∼30–50 organisms), leaving no room for additive effects. This ceiling effect reveals that criteria damage overlapping subsystems.

Growth–reproduction confound. The (reproduction, growth) pair confirms: $\Delta_{AB} = \Delta_{\text{reproduction}} = 290.4$, so growth's effect is fully mediated through reproduction gating. This clarifies growth's role as an upstream prerequisite for reproductive competence rather than an independent viability mechanism.

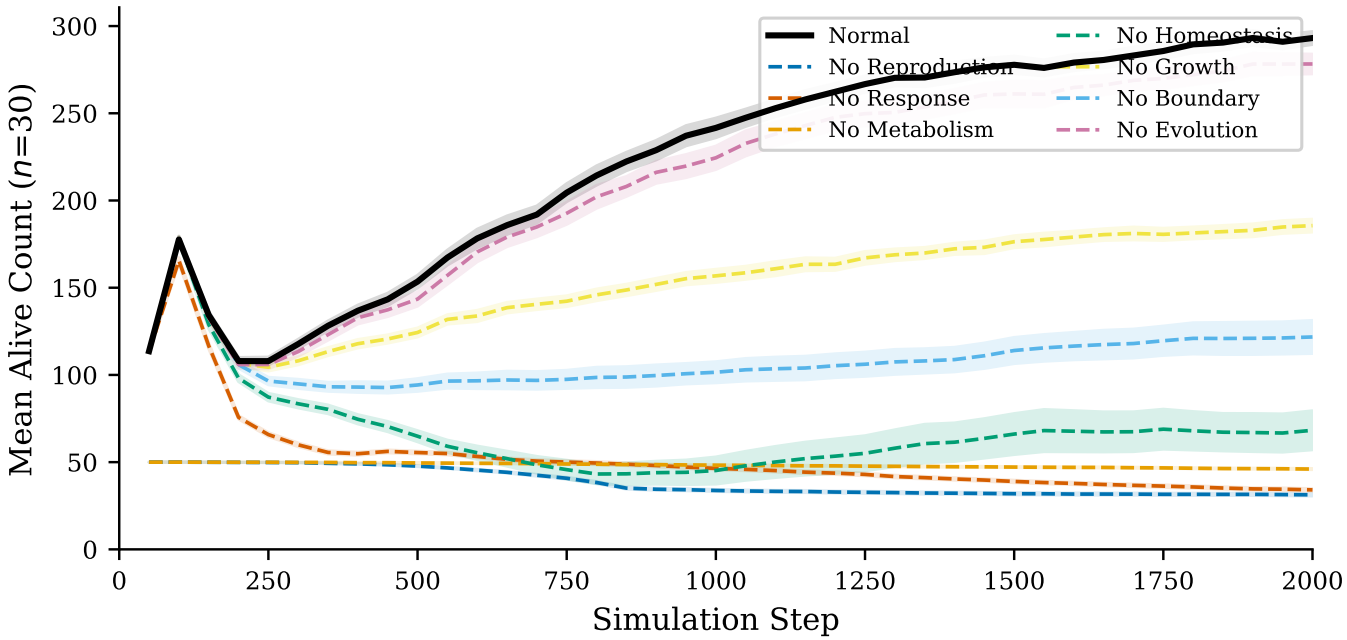

Figure 2: Population dynamics under criterion ablation. Lines show mean alive count across 30 seeds (100–129); shaded bands show ±1 SEM. Normal baseline (thick black) stabilizes near 293 organisms. Removing reproduction, response, or metabolism causes >84% population collapse. Evolution ablation shows a modest 5% decline (d=0.57), consistent with optimization rather than short-term survival necessity.

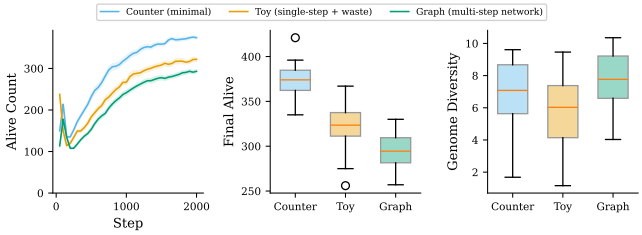

Figure 3: Proxy control comparison. Three metabolism implementations of increasing complexity on the same seeds (n=30). Graph metabolism sustains fewer organisms but higher genome diversity and waste dynamics, demonstrating that metabolic complexity produces qualitatively distinct ecological dynamics rather than simply increasing population counts.

Evolution Strengthening

The modest single-ablation effect of evolution (d=0.57, Cliff's δ=0.18) reflects the 2000-step simulation horizon. To demonstrate evolution's contribution at longer timescales, we run two additional experiments:

Long run. Extending simulations to 10,000 steps (n=30) yields d=1.46, Cliff's δ=0.72 ($p < 0.001$), a large effect compared to the modest 2000-step result. Normal populations reach $\bar{x}$=358.1 organisms versus 327.1 for no-evolution (Δ=−8.7%), confirming that evolutionary adaptation accumulates across generations.

Environmental shift. At step 2,500 of a 5,000-step simulation, resource regeneration rate is halved (from 0.01 to 0.005 per cell per step). Evolved populations recover more effectively ($\bar{x}$=384.6 vs. 361.4, d=1.02, Cliff's δ=0.57, $p < 0.001$), demonstrating that evolution enables adaptive response to environmental perturbation.

Homeostatic Regulation

Figure 5 shows population-mean internal state trajectories for Normal versus No Homeostasis conditions. Under normal operation, the neural-network controller actively regulates internal state variable s_0, maintaining it near ∼0.99 throughout the simulation (Panel A, solid line). When homeostasis is disabled, s_0 decays monotonically due to the passive decay term ($h_{\text{decay}} = 0.01$ per step), and the population exhibits high variance as organisms lack the ability to counteract perturbations (Panel B, dashed line). This divergence confirms that the NN-driven homeostatic mechanism constitutes an active regulatory process—not a static parameter—that satisfies the functional-analogy requirement of sustained resource consumption with measurable degrada-

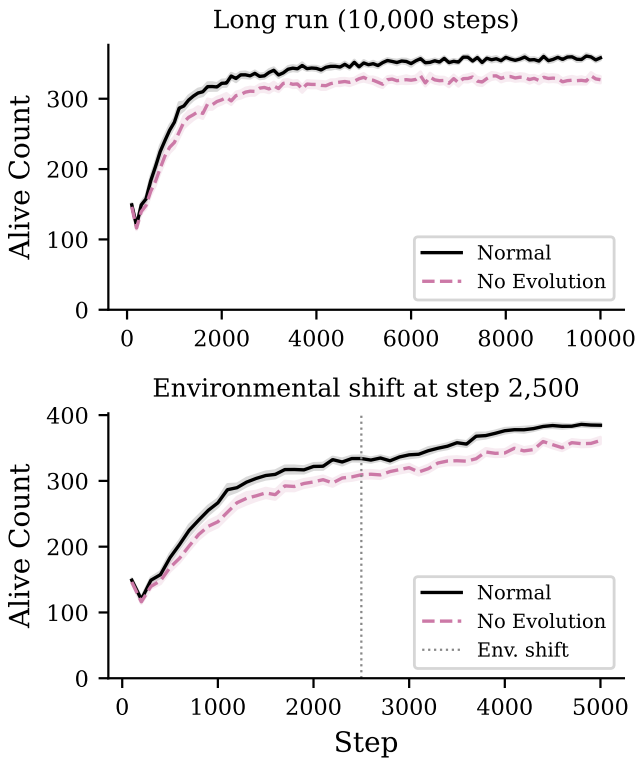

Figure 4: Evolution strengthening. Top: 10,000-step long run shows increasing divergence between normal and no-evolution conditions. Bottom: environmental shift at step 2,500 (dashed line) demonstrates evolved populations' superior recovery. Lines show mean across 30 seeds; shaded bands ±1 SEM.

tion upon removal.

Discussion

Criterion interdependence. Single ablations reveal a hierarchy: reproduction, response, and metabolism form an essential triad (>84% decline), while homeostasis and boundary occupy a middle tier (∼58–77%). Pairwise ablations show uniformly sub-additive interactions (Table 4), consistent with shared failure pathways rather than independent modules—criteria converge on overlapping viability subsystems. The proxy control comparison further demonstrates that the specific implementation of a criterion shapes ecological dynamics (graph metabolism produces higher diversity but lower populations than simpler alternatives), ruling out tautological definitions.

Evolution at longer timescales. The modest 2000-step evolution effect (d=0.57) grows to d=1.46 at 10,000 steps and d=1.02 under environmental perturbation, confirming that evolutionary adaptation accumulates

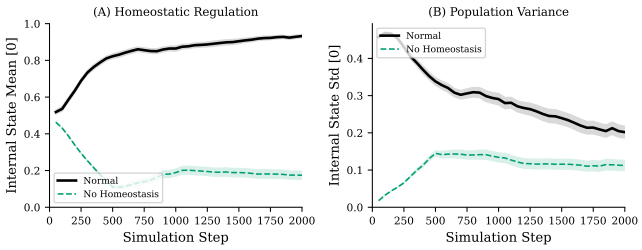

Figure 5: Homeostatic regulation trajectories (n=30). (A) Mean internal state variable s_0 over time: Normal condition (solid) maintains regulation near 1.0, while No Homeostasis (dashed) shows passive decay. (B) Population-level standard deviation of s_0: disabled homeostasis produces higher inter-organism variance. Shaded bands show ±1 SEM.

across generations.

Limitations

Growth uses a maturation toggle rather than a full developmental program; a morphogenetic model would strengthen this criterion's functional-analogy claim. Evolution reaches d=1.46 at 10,000 steps but demonstrating open-ended dynamics would require 10^5+ steps with novelty metrics (Bedau et al., 2000). Scale is limited to ∼300 organisms on a single machine; larger populations might reveal emergent ecological phenomena. We adopt a weak ALife stance: this is a functional model, not a claim that digital organisms are alive.

Conclusion

We presented a testable integration of all seven textbook biological criteria as functionally interdependent processes within a single artificial life system, verified through controlled criterion-ablation, pairwise interaction, and proxy control experiments. The functional-analogy framework—requiring dynamic operation, measurable degradation upon removal, and feedback coupling—provides a rigorous standard distinguishing genuine criteria implementations from simplified proxies.

Our results demonstrate that no criterion is decorative: removing any one causes statistically significant population decline ($p < 0.016$, Holm-Bonferroni corrected), with Cliff's δ ranging from 0.18 to 1.00. Pairwise ablations further reveal shared failure pathways—sub-additive interactions consistent with criteria converging on overlapping viability subsystems rather than operating independently.

Future work will pursue three directions: (1) a richer developmental program replacing the current growth toggle; (2) scaling to larger populations to investigate

emergent ecological phenomena and open-ended evolution metrics (Bedau et al., 2000; Taylor et al., 2016); and (3) systematic environmental perturbation studies to characterize adaptive capacity across evolutionary timescales.

Code and data will be made available upon acceptance at an anonymous repository.

References

Barbieux, A. and Canaan, R. (2024). Coralai: Intrinsic evolution of embodied neural cellular automata ecosystems. In The 2024 Conference on Artificial Life, ALIFE 2024. MIT Press.

Bedau, M. A., McCaskill, J. S., Packard, N. H., Rasmussen, S., Adami, C., Green, D. G., Ikegami, T., Kaneko, K., and Ray, T. S. (2000). Open problems in artificial life. Artificial Life, 6(4):363–376.

Chan, B. W.-C. (2019). Lenia: Biology of artificial life. Complex Systems, 28(3):251–286.

Cliff, N. (1993). Dominance statistics: Ordinal analyses to answer ordinal questions. Psychological Bulletin, 114(3):494–509.

Cohen, J. (1988). Statistical Power Analysis for the Behavioral Sciences. Routledge, 2nd edition.

Heinemann, C. (2008). Artificial life environment. Informatik-Spektrum, 31(1):55–61.

Holm, S. (1979). A simple sequentially rejective multiple test procedure. Scandinavian Journal of Statistics, 6(2):65–70.

Joyce, G. F. (1994). Foreword. In Deamer, D. W. and Fleischaker, G. R., editors, Origins of Life: The Central Concepts, pages xi–xii. Jones and Bartlett, Boston.

Mann, H. B. and Whitney, D. R. (1947). On a test of whether one of two random variables is stochastically larger than the other. The Annals of Mathematical Statistics, 18(1):50–60.

Maturana, H. R. and Varela, F. J. (1980). Autopoiesis and Cognition: The Realization of the Living. Boston Studies in the Philosophy and History of Science. Springer Netherlands.

McMullin, B. (2004). Thirty years of computational autopoiesis: A review. Artificial Life, 10(3):277–295.

Ofria, C. and Wilke, C. O. (2004). Avida: A software platform for research in computational evolutionary biology. Artificial Life, 10(2):191–229.

Plantec, E., Hamon, G., Etcheverry, M., Oudeyer, P.-Y., Moulin-Frier, C., and Chan, B. W.-C. (2023). Flow-lenia: Towards open-ended evolution in cellular automata through mass conservation and parameter localization. In The 2023 Conference on Artificial Life, ALIFE 2023. MIT Press.

Ray, T. S. (1991). An approach to the synthesis of life. In Langton, C. G., Taylor, C., Farmer, J. D., and Rasmussen, S., editors, Artificial Life II, volume XI of Santa Fe Institute Studies in the Sciences of Complexity, pages 371–408, Redwood City, CA. Addison-Wesley.

Ruiz-Mirazo, K., Peretó, J., and Moreno, A. (2004). A universal definition of life: Autonomy and open-ended evolution. Origins of Life and Evolution of the Biosphere, 34(3):323–346.

Taylor, T., Bedau, M., Channon, A., Ackley, D., Banzhaf, W., Beslon, G., Dolson, E., Froese, T., Hickinbotham, S., Ikegami, T., McMullin, B., Packard, N., Rasmussen, S., Virgo, N., Agmon, E., Clark, E., McGregor, S., Ofria, C., Ropella, G., Spector, L., Stanley, K. O., Stanton, A., Timperley, C., Vostinar, A., and Wiser, M. (2016). Open-ended evolution: Perspectives from the OEE workshop in York. Artificial Life, 22(3):408–423.

Urry, L. A., Cain, M. L., Wasserman, S. A., Minorsky, P. V., and Reece, J. B. (2020). Campbell Biology. Pearson, New York, 12th edition.

Yaeger, L. S. (1994). Computational genetics, physiology, metabolism, neural systems, learning, vision, and behavior or PolyWorld: Life in a new context. In Langton, C. G., editor, Artificial Life III, pages 263–298, Redwood City, CA. Addison-Wesley.